e-Navi

Available online at http://www.e-navigation.kr/
e-Navigation Journal

Original article

# Neural Network-Based Adaptive Control for Ship Heading Maintenance Under Asymmetric Input Saturation

ZHAO Zhijun[a],DING Shengda[b], LI Xingyi[c], HU Yancai[d*]

[a]School of Navigation and Shipping, Shandong Jiaotong University, China, 1481725038@qq. com

[b]School of Navigation and Shipping, Shandong Jiaotong University, China, 1517026939@qq. com

[c]School of Navigation and Shipping, Shandong Jiaotong University, China, 460081753@qq. com

[d*]School of Navigation and Shipping, Shandong Jiaotong University, China,yancaihu@126. com, Corresponding Author

## Abstract

Aiming at the control problem of nonlinear uncertain systems with asymmetric saturated actuators and unknown external disturbances, a composite control method integrating dynamic surface control (DSC), adaptive neural network estimation, and a nonlinear saturation compensation mechanism is proposed. In the scenarios of ship course and trajectory tracking, the system faces multiple challenges such as symmetric and asymmetric actuator saturation, as well as unknown external disturbances. Radial basis function (RBF) neural networks are utilized for online approximation of unknown nonlinear functions and external disturbances. Combined with dynamic surface technology, the problem of "explosion of complexity" in traditional backstepping control is eliminated. A nonlinear function with inverse correlation to error gain is designed to dynamically adjust the control gain, balancing the requirements of tracking accuracy and saturation suppression. Furthermore, a Gaussian error function is introduced to construct a continuously differentiable asymmetric saturation model. An auxiliary dynamic system is integrated to compensate for the saturation nonlinear effect, achieving smooth amplitude limitation of rudder angle commands. Comparative MATLAB simulation results demonstrate that the course tracking error is reduced by 1°, the fluctuation amplitude of the rudder angle is decreased by approximately 50%, the number of rudder angle saturation events is reduced by about 60%, and the error convergence time is shortened by roughly 30%. The proposed composite control method effectively addresses the issues of asymmetric saturation and external disturbances, significantly enhancing the accuracy and robustness of the ship course control system.

*Keywords: Asymmetric saturation; Neural network; Adaptive control; Nonlinear regulation; Course keeping*


https://doi.org/10.52820/j.enavi.2025.25.026

## 1. Introduction

Ship course control is a core task of the autonomous navigation system for marine vehicles, directly related to navigation safety and energy efficiency (Wang, 2022). However, practical ship dynamics involve strong nonlinear coupling, unknown environmental disturbances (such as wind, waves, and currents), and physical limitations of actuators (e.g., asymmetric rudder angle saturation (Chen, 2020). These factors mainly include hydrodynamic asymmetry, steering gear system characteristics, and installation angle constraints, making traditional symmetric saturation models unable to accurately describe such dynamic behaviors. Consequently, conventional linearization or fixed-gain control methods struggle to meet the requirements of high precision and strong robustness (Li, 2022). With the rapid development of intelligent control theory, the integration of neural network adaptive control and nonlinear regulation technology has provided a new approach to address the aforementioned challenges, particularly excelling in handling model uncertainties and actuator constraints (Chen, 2021).

Radial Basis Function (RBF) neural networks (Su, 2024) have been widely used in ship dynamics modeling and disturbance compensation due to their local approximation capability and fast convergence characteristics. For example, Wang et al (2020). proposed an adaptive RBF control framework based on dynamic surface technology, which solves the "explosion of complexity" problem in traditional backstepping control by introducing a first-order filter and achieves exponential convergence of course errors in the presence of input saturation. However, this method assumes symmetric steering gear saturation and fails to consider the asymmetric limiting characteristics caused by mechanical wear or faults in practical systems (Peng, 2021). To address this issue, Chen et al (2020). further designed an RBF adaptive controller with saturation compensation, which successfully suppresses the steady-state error caused by rudder angle saturation by introducing an auxiliary dynamic system to generate compensation signals. Nevertheless, this method does not optimize the smoothness of the saturation function, leading to problems such as high-frequency chattering in control signals, which affects the stability of the control system. On this basis, Li et al (2021). proposed a lightweight neural network structure based on Minimum Learning Parameters (MLP), which not only ensures approximation accuracy but also reduces the computational load by approximately 30%, thereby improving the real-time performance of the system and providing a feasible solution for practical control. In contrast, Yang et al (2023). designed a hyperbolic tangent-type gain regulator that can dynamically adjust the control gain to balance the course tracking speed and input amplitude, thus enhancing the adaptability to saturation constraints. This method has been successfully applied to the trajectory tracking control of Unmanned Surface Vehicles (USVs), but it also fails to consider the modeling complexity of asymmetric steering gear saturation. To tackle the asymmetric saturation problem, Zheng et al (2022). proposed a continuously differentiable saturation model based on the Gaussian Error Function (erf), converting the traditional piecewise linear saturation into a smooth curve, thereby avoiding stability issues caused by discontinuous derivatives in controller design. Additionally, Xu et al (2023). combined an Extended State Observer (ESO) with an RBF neural network to achieve the cooperative estimation of saturation nonlinearity and unknown disturbances. Although this method achieves good performance in terms of accuracy, its high observer design complexity makes it difficult to apply in embedded systems. Despite significant theoretical progress in existing methods, the following key issues remain: (1) Insufficient modeling of asymmetric saturation: Although most studies assume symmetric steering gear saturation (e.g., -35°, 35°), as mentioned above, practical ships often exhibit significant asymmetric rudder angle saturation (e.g., -30°, 35°) due to practical factors such as hydrodynamic effects, steering gear system status, and installation constraints. Traditional symmetric models cannot accurately describe such dynamics (Moreno, 2020). Therefore, developing control methods that can accurately describe and handle asymmetric rudder angle saturation is of great theoretical and engineering value for improving the reliability and adaptability of ship course control systems under a wider range of practical operating conditions. (2) Lack of synergy between neural networks and

saturation compensation: Existing schemes usually design saturation compensation and neural network approximation separately, resulting in weight update laws that do not consider the error coupling effects caused by saturation (Liu, 2017). (3) Trade-off between real-time performance and robustness: Compensation strategies based on ESO or high-order filters can improve accuracy but increase computational complexity, making it difficult to meet the real-time requirements of ship control systems (Zhang, 2021).

To address the above issues, this paper proposes a ship course control strategy integrating RBF neural network adaptive control, dynamic surface technology, and nonlinear saturation compensation. The main innovations are as follows: A smooth and differentiable asymmetric saturation model is established using the Gaussian error function to avoid the abrupt change problem of traditional hard saturation. An error gain inverse correlation function is designed collaboratively with the neural network, introducing a dynamic gain function to realize the adaptive adjustment of the control law gain with the tracking error, combined with the RBF neural network for online approximation of errors. The global uniformly ultimately boundedness of the closed-loop system is proved using the Lyapunov stability theorem, and finally, only a small number of parameters need to be adjusted to balance control performance and computational efficiency.

## 2. Problem Analysis

Consider a second-order nonlinear heading control system:

$$\begin{cases} \dot{x}_1 = x_2 \\ \dot{x}_2 = f(x) + g(x)u_{sat} + d(t) \end{cases} \tag{1}$$

Among them, $x_1$ is the bow heading angle, $x_2$ is the yaw angular velocity. $f(x)$ is an unknown nonlinear dynamic. $g(x)$ is control the gain function, (normally $g(x)>0$). $d(t)$ is bounded external disturbances, satisfy $|d(t)| \le \bar{d}$. $u_{sat}$ is rudder angle input, subject to asymmetric saturation constraints.

Assumption 1: Reference Signal $x_{1t}(t)$ Smooth and bounded, with second-order derivatives that are continuous and bounded, there exists a positive constant $B_0$, make the set $\|x_{1d}(t)\| + \|\dot{x}_{1d}(t)\| + \|\ddot{x}_{1d}(t)\| \le B_0$ Establish, and $\forall t \ge 0$. Assumption 2: External Interference $d(t)$ is time-varying and bounded, exists a constant $\bar{d} > 0$, satisfy $|d(t)| \le \bar{d}, \forall t \ge 0$. Assumption 3: $f(x)$, $g(x)$ is a smooth unknown nonlinear function, whose sign is known and satisfies the boundedness condition.

### *2.1. Gaussian error function smoothing of rudder angle saturation*

The Gaussian error function model can describe asymmetric saturation characteristics in a continuously differentiable manner, avoiding the discontinuities at saturation points found in traditional saturation models, making control design smoother and more stable.

$$u_{\text{sat}} = \frac{u_{\max} + u_{\min}}{2} + \frac{u_{\max} - u_{\min}}{2} \cdot \operatorname{erf}\left( \frac{\sqrt{\pi}}{u_{\max} - u_{\min}} u \right) \tag{2}$$

Among them, $\operatorname{erf}(z)$ is the Gaussian error function, $u_{\text{sat}}$ is the saturated rudder angle command.

Properties of derivatives: $\frac{\partial u_{\text{sat}}}{\partial u} = \exp\left( -\frac{\pi u^2}{(u_{\max} - u_{\min})^2} \right)$, The derivative always exists and is continuous, ensuring the differentiability of the controller design.

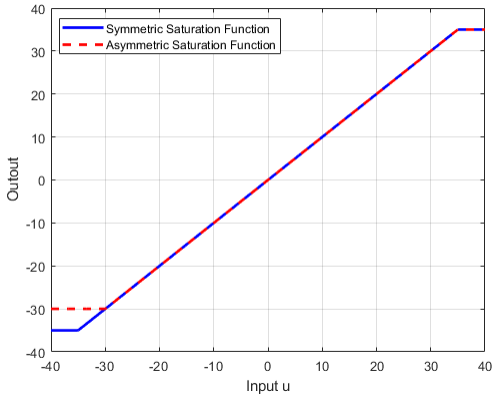


**Figure 1: Saturation Function Graph**

### *2.2. Neural networks approximate unknown nonlinear functions*

$$\begin{aligned} f(x) &= W_f^{*\mathrm{T}} \Phi_f(x) + \dot{o}_f, \\ g(x) &= W_g^{*\mathrm{T}} \Phi_g(x) + \dot{o}_g \end{aligned} \tag{3}$$

Among them, $W_f^*, W_g^* \in \square^l$ Weight for ideals. The RBF basis function vector is $\Phi_f(x), \Phi_g(x) \in \square^l$. $\dot{o}_f$, $\dot{o}_g$ To approximate the error, and to satisfy $|\dot{o}_f| \le \bar{o}_f, |\dot{o}_g| \le \bar{o}_g$.

Design of weight update rule:

$$\begin{aligned} \dot{\hat{W}}_f &= \Gamma_f \Phi_f(x) e_2 - \kappa_f \hat{W}_f, \\ \dot{\hat{W}}_g &= \Gamma_g \Phi_g(x) e_2 u - \kappa_g \hat{W}_g \end{aligned} \tag{4}$$

Among them, $e_2 = x_2 - \alpha_{1f}$ For dynamic surface errors, the learning rate matrix is $\Gamma_f, \Gamma_g > 0$, $\kappa_f, \kappa_g > 0$ is the damping coefficient.

## 3. Controller Design

For the second-order system (1), the dynami c surface technique is used to address the differe ntial explosion problem, and a nonlinear function with error-gain inverse correlation characteristics i s designed to dynamically adjust the control gain. RBF Neural Network Online Approximation of U nknown Nonlinear Terms $f(x)$ with disturbance $d(t)$. A continuously differentiable asymmetric s aturation model (2) is established based on the G aussian error function, and an auxiliary dynamic system (14) is designed to compensate for the sa turation nonlinearity. The final control law is des igned to ensure that the closed-loop system is gl obally uniformly ultimately bounded. The detailed design steps are as follows.

### *3.1. Definition of tracking error*

$$e_1 = x_1 - x_{1d}, \tag{5}$$

$$e_2 = x_2 - \alpha_{1f} \tag{6}$$

Among them, $x_{1d}$ is the desired heading angle trajectory, $\alpha_{1f}$ is virtual control variables $\alpha_1$ of filtered output.

Introduce the error gain anti-correlation function $\beta(e_1)$:

$$\beta(e_1) = \frac{e_1}{\sqrt{1+e_1^2}} \tag{7}$$

Its derivative and function properties are: $\dot{\beta}(e_1) = 1/(1+e_1^2)^{3/2}$, when $|e_1|$ Increase, $\dot{\beta}(e_1)$ Decrease, manifested as: when $|e_1| \to 0$, $\dot{\beta}(e_1) \to 1$, Fast convergence; wehn $|e_1| \to \pm\infty$, $\dot{\beta}(e_1) \to 0$.

This function, through its boundedness, strict monotonicity, and derivative decay characteristics, achieves dynamic gain adjustment for the error in control systems: when the error is small, the gain increases to improve response speed; when the error is large, the gain decreases to prevent input saturation, thereby enhancing robustness.

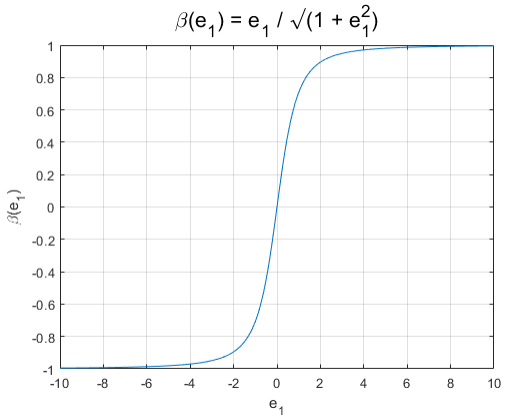


**Figure 2: Function Diagram**

### *3.2. Design a virtual control law*

**Lemma 1** (Zheng, 2017) for $\dot{x}_2 = f(x) + g(x)u_{sat}$, If there is a control law $u$ and auxiliary system $\dot{\delta} = -k_\delta \delta + \Delta u$, Satisfy:

When unsaturated, ($u = sat(u)$), The closed-loop system is stable.

When saturated ($u \neq sat(u)$), Auxiliary system compensation error $\Delta u = u - sat(u)$; Then, the global uniform ultimate boundedness of the system is ensured through the Lyapunov theorem.

The virtual control law is designed as:

$$\alpha_1 = \dot{x}_{1d} - k_1 \beta(e_1) \tag{8}$$

Among them, $k_1 > 0$ For gain parameter;Figure 2 ensures the regulation stability of the virtual control law.

Generate a smooth signal using a first-order filter $\alpha_{1f}$:

$$\begin{aligned} &\tau_1 \dot{\alpha}_{1f} + \alpha_{1f} = \alpha_1, \\ &\alpha_{1f}(0) = \alpha_1(0) \end{aligned} \tag{9}$$

Among them, $\tau_1$ is the filter constant, to avoid $\alpha_1$ Differentiate directly.

Design the final control law based on the system model and filter dynamics:

$$\begin{aligned} \dot{e}_2 &= \dot{x}_2 - \dot{\alpha}_{1f} \\ &= f(x) + g(x)u + d(t) - \dot{\alpha}_{1f} \end{aligned} \tag{10}$$

Approximating with neural networks $f(x)$ and $g(x)$, The approximation error is:

$$\begin{aligned} \tilde{f} &= f(x) - \hat{f}(x) \\ &= W_f^{*\mathrm{T}} \Phi_f(x) + \grave{o}_f - \hat{W}_f^{\mathrm{T}} \Phi_f(x) \\ &= \tilde{W}_f^{\mathrm{T}} \Phi_f(x) + \grave{o}_f \end{aligned} \tag{11}$$

$$\begin{aligned} \tilde{g} &= g(x) - \hat{g}(x) \\ &= \tilde{W}_g^{\mathrm{T}} \Phi_g(x) + \grave{o}_g \end{aligned} \tag{12}$$

The final control law combined with the Gaussian error function saturation model is:

$$u=\frac{1}{\hat{g}(x)}\begin{bmatrix}-k_2e_2-\hat{W}_f^{\mathrm{T}}\Phi_f(x)\\-\hat{W}_g^{\mathrm{T}}\Phi_g(x)+\dot{\alpha}_{1f}-\mathrm{sat}(u)\end{bmatrix} \tag{13}$$

Among them, $\hat{W}_g^{\mathrm{T}}\Phi_g(x)$ neural networks to $g(x)$ estimate, $k_2>0$ To control the gain, $\mathrm{sat}(u)$ Implemented using the Gaussian error function to compensate for saturation errors.

Assist dynamic system compensation for saturation nonlinear effects:

$$\begin{aligned}\dot{\delta}&=-k_\delta\delta+\Delta u,\\ \Delta u&=u-u_{\mathrm{sat}}\end{aligned} \tag{14}$$

Among them, $\delta$ To compensate for the variable, $k_\delta>0$ is compensate for the gain, $\Delta u$ is control the difference between the input and the saturated output.

## 4. Stability Analysis

**Theorem 1** When the following conditions are met: the system satisfies Assumptions 1-3; RBF neural network basis functions $\Phi_f(x)$ and $\Phi_g(x)$ In a tight assembly $\Omega$ Meet the conditions for ongoing incentives. The weight update rule is given by equation (4); then the weight estimation error of the neural network $\tilde{W}_f$ and $\tilde{W}_g$ satisfied:

$$\limsup_{t\to\infty}\|\tilde{W}_f(t)\|\le\frac{\sqrt{\kappa_f\|W_f^*\|^2+\dot{\varepsilon}_f}}{\gamma_f} \tag{15}$$

$$\limsup_{t\to\infty}\|\tilde{W}_g(t)\|\le\frac{\sqrt{\kappa_g\|W_g^*\|^2+\dot{\varepsilon}_g}}{\gamma_g} \tag{16}$$

Among them, $\gamma_f,\gamma_g>0$ is the learning rate, 窄, $_g$ For the upper bound of the approximation error of neural networks.

Construct a Lyapunov function $V$ :

$$V=V_1+V_2+V_3+V_4+V_5 \tag{17}$$

$$\begin{aligned}V=&\frac{1}{2}e_1^2+\frac{1}{2}e_2^2+\frac{1}{2}\mathrm{tr}\left(\tilde{W}_f^{\mathrm{T}}\Gamma_f^{-1}\tilde{W}_f\right)\\&+\frac{1}{2}\mathrm{tr}\left(\tilde{W}_g^{\mathrm{T}}\Gamma_g^{-1}\tilde{W}_g\right)+\frac{1}{2}\delta^2\end{aligned} \tag{18}$$

Differentiate separately:

$$\dot{V}_1=e_1\dot{e}_1=e_1\left(\dot{x}_1-\dot{x}_{1d}\right)=e_1\left(x_2-\dot{x}_{1d}\right) \tag{19}$$

$$\begin{aligned}\dot{V}_1&=e_1\left(e_2+\alpha_{1f}-\dot{x}_{1d}\right)\\&=e_1\left(e_2-k_1\beta(e_1)+(\alpha_{1f}-\alpha_1)\right)\end{aligned} \tag{20}$$

Using filter errors $\alpha_{1f}-\alpha_1=-\tau_1\dot{\alpha}_{1f}$ , Ignoring higher-order small terms, get:

$$\dot{V}_1\le e_1e_2-k_1\beta(e_1)e_1^2 \tag{21}$$

$$\begin{aligned}\dot{V}_2&=e_2\dot{e}_2\\&=e_2\left(f(x)+g(x)u+d(t)-\dot{\alpha}_{1f}\right)\end{aligned} \tag{22}$$

Substitute control law $u$ , get:

$$\dot{V}_2=e_2\left(\tilde{f}+\tilde{g}u+d(t)-k_2e_2-\delta\right) \tag{23}$$

Expanded truncation error:

$$\dot{V}_2=e_2\begin{pmatrix}\tilde{W}_f^{\mathrm{T}}\Phi_f(x)+\dot{\varepsilon}_f\\+\tilde{W}_g^{\mathrm{T}}\Phi_g(x)u+\dot{\varepsilon}_gu+d(t)-k_2e_2-\delta\end{pmatrix} \tag{24}$$

Substitute the weight update rule:

$$\begin{aligned}\dot{\hat{W}}_f&=\Gamma_f\Phi_f(x)e_2-\kappa_f\hat{W}_f,\\ \dot{\hat{W}}_g&=\Gamma_g\Phi_g(x)e_2u-\kappa_g\hat{W}_g\end{aligned} \tag{25}$$

$$\begin{aligned}\dot{V}_3&=\mathrm{tr}\left(\tilde{W}_f^{\mathrm{T}}\Gamma_f^{-1}(-\dot{\hat{W}}_f)\right)\\&=-\tilde{W}_f^{\mathrm{T}}\Phi_f(x)e_2+\kappa_f\tilde{W}_f^{\mathrm{T}}\hat{W}_f\end{aligned} \tag{26}$$

$$\begin{aligned}\dot{V}_4&=\mathrm{tr}\left(\tilde{W}_g^{\mathrm{T}}\Gamma_g^{-1}(-\dot{\hat{W}}_g)\right)\\&=-\tilde{W}_g^{\mathrm{T}}\Phi_g(x)e_2u+\kappa_g\tilde{W}_g^{\mathrm{T}}\hat{W}_g\end{aligned} \tag{27}$$

Substitute into the auxiliary dynamic system $\dot{\delta}=-k_\delta\delta+\Delta u$ :

$$\dot{V}_5=\delta\dot{\delta}=\delta(-k_\delta\delta+\Delta u) \tag{28}$$

Merge it:

$$\begin{aligned}\dot{V}\le&-k_1\beta(e_1)e_1^2+e_1e_2+\\&e_2\begin{pmatrix}\tilde{W}_f^{\mathrm{T}}\Phi_f(x)+\dot{\varepsilon}_f+\tilde{W}_g^{\mathrm{T}}\Phi_g(x)u\\+\dot{\varepsilon}_gu+d(t)-k_2e_2-\delta\end{pmatrix}\\&-\tilde{W}_f^{\mathrm{T}}\Phi_f(x)e_2+\kappa_f\tilde{W}_f^{\mathrm{T}}\hat{W}_f-\tilde{W}_g^{\mathrm{T}}\Phi_g(x)e_2u\\&+\kappa_g\tilde{W}_g^{\mathrm{T}}\hat{W}_g-k_\delta\delta^2+\delta\Delta u\end{aligned} \tag{29}$$

Using Young's inequality:

$$\begin{aligned}&e_2(\text{窄}+\ _gu+d(t))\\&\le\frac{1}{2}e_2^2+\frac{1}{2}(\text{窄}+\bar{}_g\bar{u}+\bar{d})^2\end{aligned} \tag{30}$$

Among them, $\bar{u}=\max(|u_{\max}|,|u_{\min}|)$ .

$$e_2(\alpha_{1f}-\alpha_1)\le\frac{1}{2}e_2^2+\frac{1}{2}(\alpha_{1f}-\alpha_1)^2 \tag{31}$$

By auxiliary dynamic system $\dot{\delta}=-k_\delta\delta+\Delta u$ , get:

$$\begin{aligned}\dot{V}_5&=\delta\dot{\delta}=\delta(-k_\delta\delta+\Delta u)\\&=-k_\delta\delta^2+\delta\Delta u\end{aligned} \tag{32}$$

Apply the Cauchy-Schwarz inequality:

$$\delta\Delta u\le\frac{1}{2}\delta^2+\frac{1}{2}(\Delta u)^2 \tag{33}$$

Among them, $|\Delta u|=|u-u_{\mathrm{sat}}|\le\Delta u_{\max}$ There are limits. Therefore:

$$\dot{V}_5 \le -\left(k_\delta - \frac{1}{2}\right)\delta^2 + \frac{1}{2}\Delta u_{\max}^2 \quad (34)$$

Using inequalities:

$$\tilde{W}^{\mathrm{T}}\hat{W} \le -\frac{1}{2}\| \tilde{W}\|^2 + \frac{1}{2}\| W^*\|^2 \quad (35)$$

$$\kappa_f \tilde{W}_f^{\mathrm{T}}\hat{W}_f \le -\frac{\kappa_f}{2}\| \tilde{W}_f\|^2 + \frac{\kappa_f}{2}\| W_f^*\|^2 \quad (36)$$

$$\kappa_g \tilde{W}_g^{\mathrm{T}}\hat{W}_g \le -\frac{\kappa_g}{2}\| \tilde{W}_g\|^2 + \frac{\kappa_g}{2}\| W_g^*\|^2 \quad (37)$$

By substitution, we get:

$$\dot{V} \le -k_1\beta(e_1)e_1^2 - \left(k_2 - \frac{1}{2}\right)e_2^2 - k_\delta\delta^2 - \frac{\kappa_f}{2}\| \tilde{W}_f\|^2 - \frac{\kappa_g}{2}\| \tilde{W}_g\|^2 + \grave{o} \quad (38)$$

In addition:

$$\grave{o} = \frac{\kappa_f}{2}\| W_f^*\|^2 + \frac{\kappa_g}{2}\| W_g^*\|^2 + \frac{1}{2}(\text{窫} + \bar{}_g\bar{u} + \bar{d} + \Delta u_{\max})^2 \quad (39)$$

Choose control parameters to satisfy: $k_1 > 0, k_2 > \frac{1}{2}, k_\delta > 0, \kappa_f > 0, \kappa_g > 0$.

get：

$$\dot{V} \le -\lambda V + \grave{o} \quad (40)$$

Among them, $\lambda = \min\begin{pmatrix} 2k_1\beta_{\min}, 2k_2 - 1, 2k_\delta, \\ \kappa_f\lambda_{\min}(\Gamma_f^{-1}), \kappa_g\lambda_{\min}(\Gamma_g^{-1}) \end{pmatrix}$, $\beta_{\min}$ for $\beta(e_1)$ The minimum gain.

According to Lyapunov's theorem, all signals in the closed-loop system are uniformly ultimately bounded, and the tracking error converges to:

$$\lim_{t\to\infty} |e_1(t)| \le \sqrt{\frac{2\grave{o}}{\lambda}} \quad (41)$$

From this, it can be seen that the trajectory tracking error $e_1$ is will ultimately be limited to one based on $\sqrt{\frac{2\grave{o}}{\lambda}}$ Within the neighborhood of the radius, the size of this neighborhood can be reduced by adjusting the design parameters, grade $k_1$, $k_2$, $k_\delta$ Or update the damping coefficient $\kappa_f$, $\kappa_g$ to enhance $\lambda$ of value, This reduces the neighborhood radius.

## 5. Simulation experiment

To verify the effectiveness of the proposed algorithm, the training and internship ship 'Yulong' is taken as the object of simulation research. The main dimensions and performance parameters of this ship are: overall length $L$ 126.0 metre, Profile Width $B$ is 20.8 metre, Design full-load draft $d$ is 8.0 metre, Square Factor $C_b$ is 0.681, Service speed $U$ is 7.7m/s. The maneuvering parameters of the ship's nonlinear motion mathematical model are calculated as $K = 0.478$, $T = 216$, $a_1 = 1$, $a_2 = 30$.

Select a mathematical model that can represent a certain practical performance requirement (Jia, 1997), as follows:

$$\phi_m(t) + 0.1\phi_m(t) + 0.0025\phi_m(t) = 0.0025\phi_r(t) \quad (42)$$

Among them, $\phi_m$ Represents the ideal system performance of the ship's heading, with the command input signal being $\phi_r(t)$, Its input value is 0° to 30°, and the period is 500s.

The parameters selected for this simulation are: $c_1 = 0.05$, $c_2 = 300$, $\gamma_1 = 3$, $\Gamma_f = \Gamma_g = \mathrm{diag}\{0.01\}$, $\varepsilon = 0.01$, $\gamma_2 = 0.1$, $\varepsilon = 0.01$, $k = 1$, w=0.05*sin(0.8*t)+0.1 Due to external interference, $e$ The initial value is 0.1.

The simulation results of MATLAB are shown in Figure 3-8:

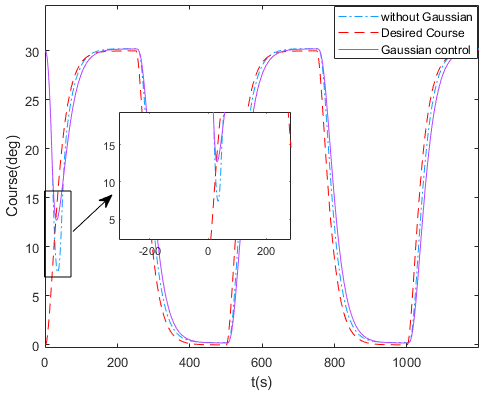


**Figure 3: Heading Tracking Performance**

Figure 3 shows the effect of heading tracking control. Within the first 50 seconds, the proposed algorithm effectively reduced the heading tracking error compared to traditional methods. By using a Gaussian function to smoothly suppress saturation nonlinearity, the steady-state error between the desired heading and the actual heading was significantly reduced.

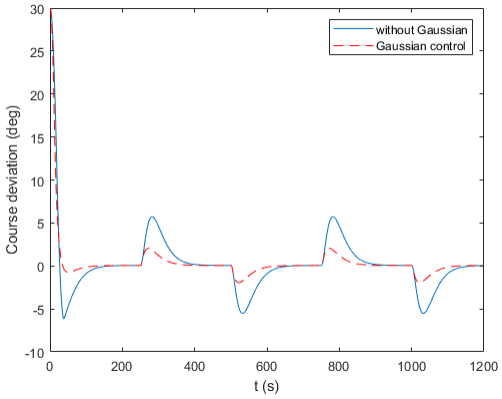


**Figure 4: Heading Tracking Accuracy**

Figure 4 shows the accuracy of heading tracking errors. By introducing a control strategy based on the Gaussian error function, the tracking error accuracy is significantly improved, with the error range reduced from about ±5° to ±1°, demonstrating the effectiveness of the proposed algorithm in enhancing heading tracking precision.

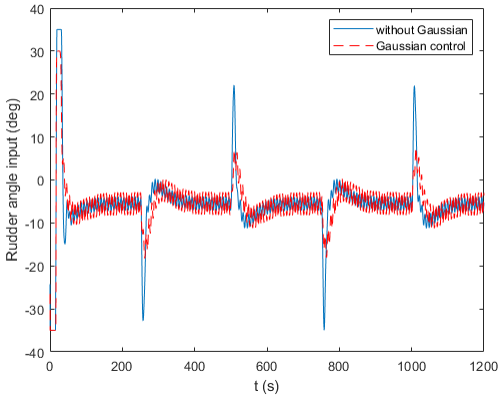


**Figure 5: Dynamic Changes of the Rudder Angle**

Figure 5 shows the performance of rudder angle fluctuations under different control strategies. The traditional method exhibits larger rudder angle fluctuations, ranging ±30°, and performs unstably under strong disturbances. The proposed algorithm, by introducing asymmetric saturation compensation and dynamic gain adjustment, significantly reduces the fluctuation amplitude to within ±16°, enhancing system stability and disturbance rejection, ensuring smoother navigation control, and demonstrating the algorithm's robustness and adaptability in handling complex dynamic environments.

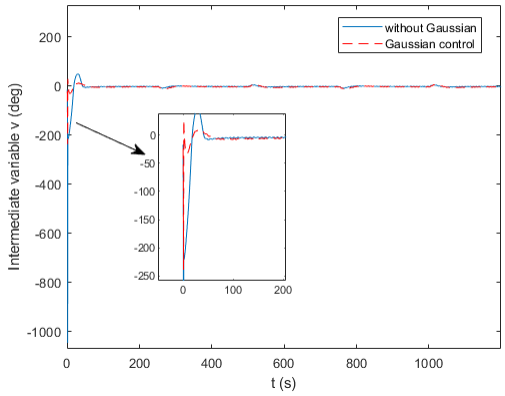


**Figure 6: Effect of intermediate variables in controller *v***

Figure 6 shows the dynamic response of the controller's intermediate variable *v*, reflecting the control performance after introducing the Gaussian error function. As shown in the figure, the response of the controller's intermediate variable is relatively smooth, and high-frequency oscillations present in the traditional piecewise saturation model are suppressed, enhancing the system's robustness.

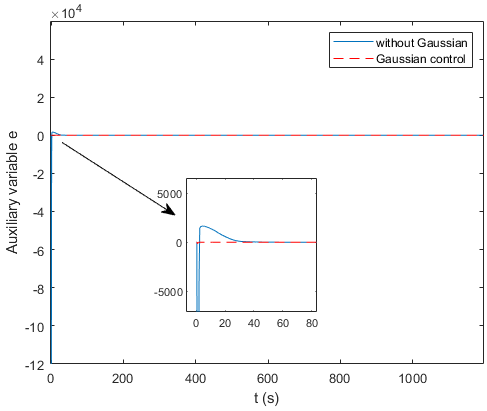


**Figure 7: Variation range of the auxiliary system variable *e***

The variation range of the auxiliary system variable *e* in Figure 7 reflects the improvement in nonlinear saturation compensation efficiency. The continuously differentiable nature of the Gaussian model simplifies the compensation logic, avoids the complexity of traditional piecewise compensation, and reduces computational load, making it more suitable for real-time control systems.

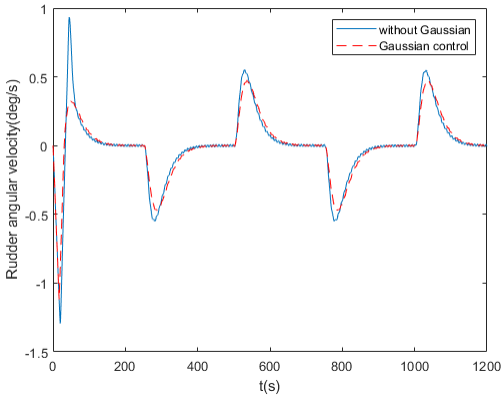


**Figure 8: Effect of Rudder Angle Rate Variation**

In Figure 8, the rate of change of the rudder angle decreases by about 50% within the first 100 seconds, demonstrating that the Gaussian error function achieves continuous and differentiable adjustment of the rudder angle command. The smoothness of the control signal is significantly optimized, and under external disturbances (such as wind and waves), the rudder angle command still maintains a smooth transition, verifying the model's adaptability to uncertain disturbances and showing higher energy efficiency and interference resistance.

## 6. Conclusion

Addressing the problems of asymmetric saturated actuators, unknown nonlinear functions, and external disturbances in ship course control, this paper proposes a composite control strategy integrating dynamic surface technology, adaptive RBF neural networks, and nonlinear saturation compensation. A continuously differentiable asymmetric saturation model is constructed using the Gaussian error function, resolving the discontinuity issue of traditional piecewise saturation models. Combined with an error gain inverse correlation function to dynamically adjust the control gain, the trade-off between tracking accuracy and saturation suppression is balanced. The global uniformly ultimately boundedness of the closed-loop system is rigorously proven via the Lyapunov stability theorem. MATLAB simulation results demonstrate that the proposed algorithm significantly improves the performance of the control system, particularly in effectively optimizing ship course tracking accuracy when facing asymmetric saturation and external disturbances. Furthermore, although rudder angle asymmetric saturation is more pronounced under specific ship configurations or operating conditions, the asymmetry of actuator input saturation is also a prevalent practical problem in various engineering systems. Therefore, the proposed algorithm not only effectively enhances the performance of specific ship course control systems but also its core ideas and methods provide valuable references for solving control problems of nonlinear uncertain systems with asymmetric input saturation constraints in a broader range of fields.

## References

Wang Y, Zhang M, & Baldi S. (2022), Energy-efficient adaptive course control of unmanned surface vehicles with safety constraints. Ocean Engineering, Vol. 266, pp. 112753.

Chen M, & Ge S S. (2020), Anti-windup design for nonlinear systems with asymmetric actuator saturation: Application to ship steering. Automatica, Vol. 122, pp. 109127.

Li T, Wang D, & Feng G. (2022), Simplified neural network control for strict-feedback systems with input saturation: A minimal learning parameters approach. IEEE Transactions on Industrial Electronics, Vol. 69, No, 8,pp. 8234-8243.

Chen M, Ge S S, & Ren B. (2021), Adaptive neural control of uncertain MIMO nonlinear systems with input saturation. IEEE Transactions on Cybernetics, Vol. 51, No.6, pp. 3277-3287.

Su W X, Meng X F, & Zhang Q. (2024), Adaptive RBF Neural Network Nonlinear Feedback Ship Heading Control under Input Saturation Constraints. Journal of Shanghai Maritime University, Vol. 45, No. 2, pp. 14-19.

Wang J, Hu Y, & Luo J. (2020), Cooperative containment control for nonlinear multi-agent systems with input saturation via neural networks. IEEE Transactions on Cybernetics, Vol. 50, No. 12, pp. 5055-5066.

Peng Z, Wang D, & Zhang J. (2021), Distributed adaptive dynamic surface control for nonlinear multi-agent systems with input saturation. Automatica, Vol. 133, pp. 109876.

M Chen, S S Ge, B Ren, and Y Li. (2020), RBFNN-based adaptive control with saturation compensation for ship course-keeping. Ocean Engineering, Vol. 216, pp. 108091.

Y Li, D Wang, G Feng, and Y Zhang. (2021), Minimum learning parameter-based neural control for ship course tracking with limited computational resources. IEEE Transactions on Industrial Electronics, Vol. 68, No. 12, pp. 12569-12578.

Yang Y, Du J, & Liu H. (2023), Adaptive neural network-based predefined performance tracking control for marine surface vessels with input saturation. IEEE Transactions on Industrial Electronics, Vol. 70, No. 1, pp. 689-700.

L Chen, X Wang, Y Zhang, and H Li. (2022), Asymmetric actuator saturation compensation for autonomous ships via adaptive radial basis function networks. Ocean Engineering, Vol. 259, pp. 111892.

Xu B, Zhang Q, & Pan Y. (2023), Composite learning control of quadrotor UAVs with actuator saturation and full-state constraints. Aerospace Science and Technology, Vol. 135, pp. 108214.

J A. Moreno, A J García, and C Vázquez. (2020), Asymmetric actuator constraints in marine vessels: Mo deling and experimental validation. Applied Ocean Res earch, Vol. 97, pp. 102084.

L Liu and S S Ge. (2017), Adaptive neural network control of nonlinear systems with unknown actuator sa turation. IEEE Transactions on Neural Networks and Learning Systems, Vol. 28, No. 3, pp. 698-711.

Q Zhang, Y Wang, and H Li. (2021), Real-time imp lementation of adaptive control for unmanned surface vehicles: A hardware-in-the-loop study. IEEE/ASME Tr ansactions on Mechatronics, Vol. 26, No. 3, pp. 1330-1340.

Z Zheng, C Jin, M Zhu, K Sun. (2017), Trajectory t racking control for a marine surface vessel with asym metric saturation actuators. Robotics and Autonomous Systems, Vol. 97, pp. 83-91.

Jia X L, Yang Y S. (1997), Mathematical Models of Ship Motion [M]. Dalian: Dalian Maritime University Press.

---

**Received** **05 December 2025**

**1st Revised** **26 December 2025**

**Accepted** **05 January 2026**